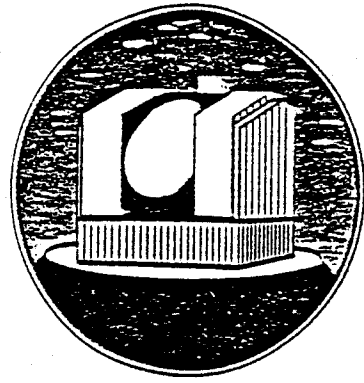
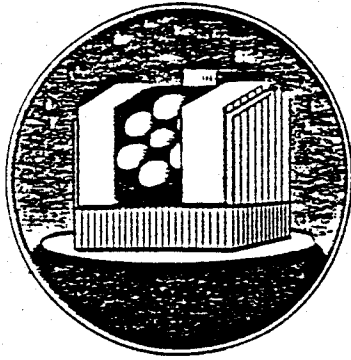


6.5 METER TELESCOPE



MMT Conversion Technical Memorandum #92-4

Interferometric Metrology for a 6.5-meter
F/1.25 Paraboloidal Mirror

James H. Burge
Steward Observatory Mirror Lab

July 15, 1992

Interferometric metrology for a 6.5-meter F/1.25 paraboloidal mirror

James H. Burge

Steward Observatory Mirror Lab
University of Arizona
Tucson, Arizona 85721
(602) 621-9595

Introduction

Optical tests have been designed and analyzed for the interferometric testing of the highly aspheric 6.5-meter F/1.25 primary mirror which was recently cast at the University of Arizona to upgrade the Multiple Mirror Telescope (MMT.) An infrared interferometer using a CO₂ laser, a null corrector, and a pyroelectric vidicon will test the surface during loose-abrasive grinding. Precision metrology for the testing of the polished surface will use a visible Shack-cube interferometer co-aligned with a BK7 null corrector, a HeNe laser source, imaging optics, and a CCD array. Both the infrared and visible systems have been carefully designed to give excellent performance in terms of wavefront correction, alignment sensitivity, imaging of the mirror to the detector, diffraction effects, ghost reflections, and ease of use.

Optical Metrology Using Null Correctors

The principle behind both interferometric systems is the same. The laser light is split into a reference beam, which is shifted in phase using a piezo-electric transducer, and a test beam. The null corrector¹ is constructed to modify the test beam to produce a wavefront that matches the desired shape of the mirror. This wavefront reflects off the mirror, picking up any figure errors, and reverses its path through the null corrector to the interferometer. The test beam is coherently added to the reference beam resulting in an interference fringe pattern that corresponds to the phase difference between the two beams. The interference fringes are projected onto a detector and

digitized for analysis. By simultaneously shifting the reference beam and measuring the change in intensity at each pixel, the phase difference, which is proportional to the surface error of the mirror, is calculated at each sampled location.

Since this process measures phase difference between two wavefronts and attributes it entirely to the surface of the mirror under test, errors in both wavefronts are kept to an absolute minimum. The null correctors were designed such that they can be fabricated and yield an uncertainty within an allotted error budget.

During grinding and polishing, the metrology data will be used to direct the figuring. It is important for the mapping distortion of the mirror through the null lens to be minimal so that the opticians can accurately address the figure errors. The infrared null lens was designed to have minimal mapping error and the visible system uses relay optics to correct the distortion introduced by the null lens.

Since the interferometry requires coherent light, diffraction from the edge of the mirror (which is the system aperture) can cause errors in the measurement. This error is minimized by focusing the image of the aperture onto the detector array. Since the very edge of the mirror is often rolled, defining this focus is difficult in practice. Both of the interferometers will use apertures at intermediate images of the primary to help define the focus. Also, a rotating ground glass disk correctly positioned in the visible system will eliminate Fresnel noise which is caused by scatter of the coherent laser light by dust particles. Both null correctors were designed so that no ghost reflections will cause troublesome spurious fringes.

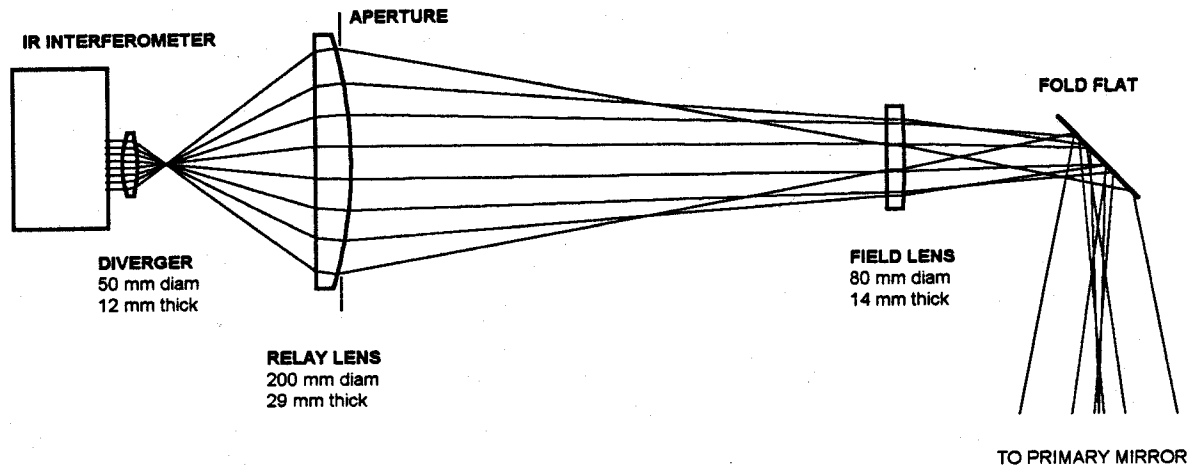


Fig. 1. Optical layout of the infrared null lens and interferometer.

Interferometry with Infrared Light

The mirror surface will be generated to an accuracy of about $5 \mu\text{m rms}$, then it will be lapped with loose abrasives to about $0.5 \mu\text{m rms}$. An infrared phase-shifting Twyman-Green interferometer with a null corrector will be used to measure the ground surface. The interferometer, made by Breault Research Organization, uses a CO_2 laser operating at $10.6 \mu\text{m}$, a PZT-shifted reference mirror, and a pyroelectric vidicon detector. The null lens will be aligned to the collimated test beam and rigidly coupled to the interferometer. The null corrector shown in Fig. 1 consists of three lenses: an aspheric ZnSe diverger, a plano-convex germanium relay lens, and a plano-convex ZnSe field lens. The optical design gives a wavefront error of $0.014 \mu\text{m rms}$ and maximum mapping error of 1.3%. The null corrector will be mounted horizontally to machine tolerances. The relative alignment between the system and the mirror will be performed by translating the interferometer-null corrector in three directions and steering the beam with a fold flat. A small aperture at the focus of the diverger will reduce stray light.

By using a single diamond-turned aspheric surface, both wavefront correction and imaging performance are optimized. The relative sizes of the elements are the smallest that will work when aligned to machine tolerances (about $50 \mu\text{m}$ over 200 mm.) A thorough tolerance analysis of the system indicates that it will contribute surface measurement errors of $1.5 \mu\text{m rms}$; however, most of this error will be measured using a rotation test and subtracted.

In order to avoid the diffraction problems associated with infrared interferometry, the image of the primary mirror is accurately focused onto the

vidicon. To facilitate this, the null corrector creates a real image of the primary mirror very near the large relay lens, where a circular aperture is accurately placed. This provides a sharp aperture to define the focus.

Interferometry with Visible Light

Once the loose abrasive grinding is complete, the mirror surface will be polished to an accuracy of about 20 nm rms . A visible wavelength phase-shifting Shack-cube interferometer with a null corrector will be used to measure the polished surface. The interferometer uses a HeNe stabilized laser operating at 632.8 nm , a PZT-shifted Shack cube, imaging optics, and shuttered CCD detector. The Shack-cube and null lens will be precisely aligned to a single rigid truss². The null corrector shown in Fig. 2 consists of the Shack-cube and three BK7 lenses: a relay lens, and two field lenses. The optical design gives a wavefront error of 5 nm rms (Fig. 3) and maximum mapping error of almost 5%. The null corrector will be mounted vertically to precision tolerances. The relative alignment between the system and the mirror will be performed by translating the entire unit in three directions and rotating about two flex-pivots. This alignment will be controlled remotely from a testing station which is not on the vibration-isolated test tower.

The telescope error budget was performed with the goal of specifying the components such that the system will not degrade the imaging performance under the best seeing conditions³. Since the atmosphere is easily characterized using structure functions, it is useful for the telescope error budget to use them also. Structure functions, which are defined as mean square phase

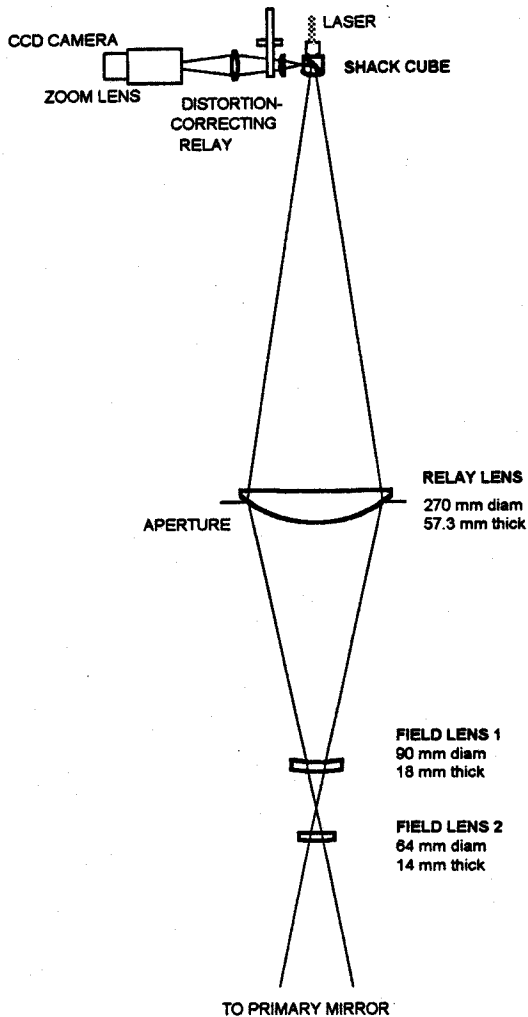


Fig. 2. Optical layout of the visible null lens with Shack-cube interferometer and distortion-correcting relay.

difference for points on the mirror as a function of point spacing, contain more information than single numbers such as rms surface error or FWHM image size. Structure functions are easily computed, and since they are mean square phase differences, the cumulative effects of independent parameters are found by simply adding their structure functions. Other functions that statistically specify optical surfaces such as autocorrelations and power spectral densities are closely related to structure functions.

In order to directly relate to the telescope error budget, structure functions are used for the tolerance analysis of the null corrector. The telescope error budget allotted the testing of the primary mirror a structure function corresponding to an r_0 of 270 cm (which gives atmospheric seeing of 0.04 arc-sec FWHM). The specification assumed the removal of

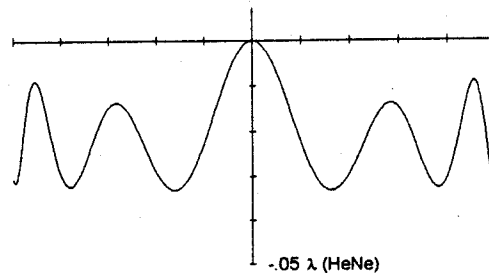


Fig. 3. OPD for visible null lens.

tilt from the wavefront and relaxation at small spatial scales corresponding to 0.25% diffracted energy loss at 350 nm wavelength.

The tolerance analysis of the interferometric test was performed by computing structure functions for all of the independent parameters in the system and adding them up⁴. Structure functions for uncertainties in all direct dimensions (spacings, curvatures, refractive index, misalignments, etc.) were computed by ray-trace simulation and analysis of the system. Realistic measurement uncertainties that have been achieved on previous null optics were assumed. Structure functions from the surface figures of the optical elements were estimated by using data from finished optical surfaces. Refractive index inhomogeneity structure functions were estimated for H5 quality glass by using melt data and assuming a linear dependence of rms phase error on point separation. The structure functions from all parameters in the null test were added to give the total test optics structure function shown in figure 4. The analysis does not take into account the ability to measure and remove azimuthal errors.

Distinct from the structure function requirement is a tolerance on the conic constant of the primary. The null lens described introduces an uncertainty of the conic constant of ± 0.00012 . A scanning pentaprism test⁵ will serve as an independent verification of the radial figure.

The imaging distortion introduced by the null lens will be corrected with the relay optics that are shown in Fig. 2. A plot of the mapping error is shown in Fig. 5. This relay not only corrects the mapping error, but it projects the image of the primary to infinity. This allows the use of a standard zoom lens to re-image the pupil at varying magnification. The re-imaging system consists of a 6X zoom lens fixed to the CCD camera which is then mounted on a tip-tilt stage. All of the controls will be operated remotely to allow the test optician to magnify the image and to look with increased resolution anywhere on the mirror. High resolution (~ 6 mm) will then be attained for sub-

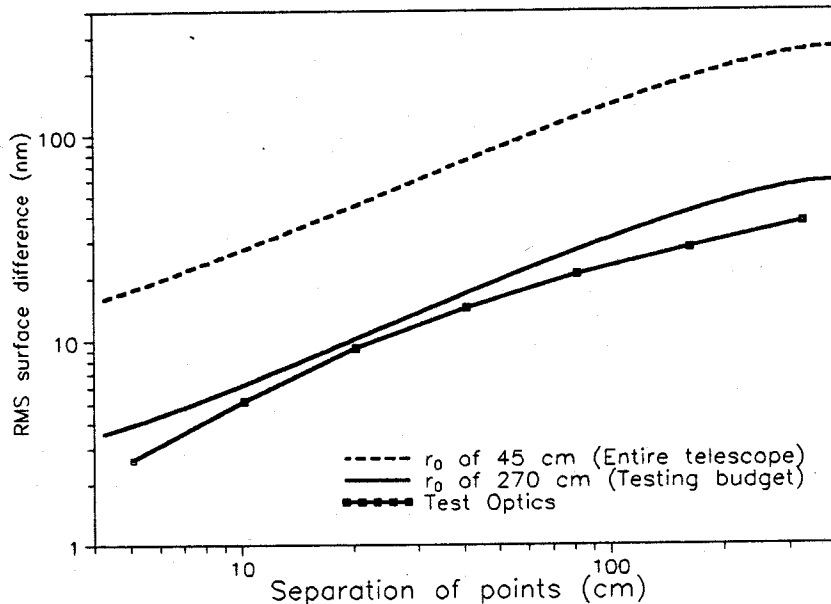


Fig. 4. Structure function from the error analysis of the visible null corrector. The telescope and test optics specifications are based on a tilt-corrected Kolmogorov model of the atmosphere with a relaxation at small spatial scales.

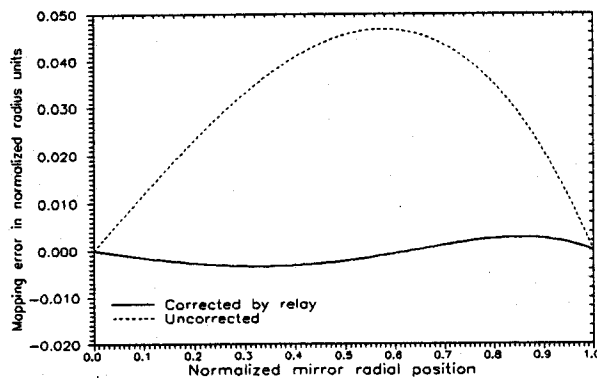


Fig. 5. Mapping error for the corrected and uncorrected visible null lens. The mapping error is in units of normalized radius for the 6.5 m primary.

aperture testing without increasing the array size, which would greatly slow processing.

As in the infrared system, the visible null corrector creates a real image of the primary mirror near the large relay lens, where a circular aperture will be accurately placed. This sharp aperture will allow the accurate focusing of the mirror onto the CCD, eliminating diffraction problems. The distortion-correcting relay also creates an intermediate real image of the primary. At this location, a rotating ground glass disk will be placed to eliminate annoying speckle and Fresnel noise.

Conclusion

The interferometric metrology for the MMT 6.5-meter F/1.25 primary mirror will accurately measure surface errors during grinding and polishing. A thorough treatment of alignment tolerances insures that the test accuracy will meet the specification. The imaging of the primary to the detector was designed to be free from mapping errors and to eliminate diffraction problems. The alignment of the interferometer relative to the primary, as well as the angular position and magnification of the imaging system will be performed from a remote test station allowing rapid collection of high-quality data.

References

- ¹A. Offner, "A Null Corrector for Paraboloidal Mirrors", *Appl. Opt.*, **2**, 153 (1963).
- ²S. C. West et al., "Optical Metrology of Two Highly Aspheric Telescope Mirrors", *Appl. Opt.*, in press, (1992).
- ³J. H. Hill, "Optical Design, Error Budget and Specifications for the Columbus Project Telescope", *Proc. S.P.I.E.*, **1236**, pp. 86-107, (1990).
- ⁴J. H. Burge, "Design and Analysis of Null Test Optics for Large Aspheric Mirrors", *Proc. ESO*, in press, (1992).
- ⁵R. N. Wilson, "Matching Error' (Spherical Aberration) in the Hubble Space Telescope (HST): Some Technical Comments", *ESO Messenger* **61**, 22 (1990).